The correlation between local defect absorbance and quasi-Fermi level splitting in CuInS2 from photoluminescence

F Heidemann, R Brüggemann, G H Bauer

Correlation between local defect absorbance and quasi-Fermi level splitting in $CuInS_2$ from photoluminescence

F. Heidemann, R. Brüggemann and G.H. Bauer

Institute of Physics, Carl von Ossietzky University, 26111 Oldenburg, Germany

E-mail: florian.heidemann@uni-oldenburg.de

Abstract. Analogously with $Cu(In,Ga)Se_2$, $CuInS_2$ shows a high degree of spatial inhomogeneities in structural, optical and electronic properties on the length scale of grain sizes and above which is caused by the grainy structure and the inhomogeneous growth of absorber layers. To analyze these locally fluctuating magnitudes, spectrally resolved photoluminescence measurements with high lateral resolution ($\leq 1\mu$m) have been performed in a confocal microscope set-up. Based on these data sets and on Planck's generalized law the determination of the spatial variation in the splitting of the quasi-Fermi levels and access to the local absorbance is possible. A detailed analysis of these properties, crucial for the solar light conversion efficiency of a final cell, is made for a $CuInS_2$ absorber layer for data obtained from statistically representative scan areas. A cross-correlation between the splitting of the local quasi Fermi levels and the local absorbance of an absorber leads to the conclusion that the splitting of quasi Fermi levels is strongly governed by the excess-carrier recombination via deep defects.

PACS numbers: 78.55.-m,73.50.Gr, 71.55.-i,78.20.-e

Submitted to: *J. Phys. D: Appl. Phys.*

1. Introduction

Chalcopyrite absorber layers are attractive for thin film photovoltaic modules. Besides $Cu(In,Ga)Se_2$ (CIGSe) absorber layers which have reached top efficiencies of $\eta \approx 20\%$ in thin film solar cells [1], the sulfidic counterpart $Cu(In,Ga)S_2$ (CIGS) or $CuInS_2$ (CIS) offers the advantage of a higher band-gap and accordingly the potential of a nominal higher open circuit voltage V_{oc} [2, 3]. However, equivalent V_{oc} have not been achieved and cell efficiencies based on CIGS and on CIS have only reached up to 13% and 11.4% so far [4, 5, 6]. Analogously with CIGSe, CIS thin films show a high degree of lateral inhomogeneities in optical, electronical and structural properties [7]. These lower the efficiency of cells and are caused by their manufacturing process [8]. A detailed analysis of such inhomogeneities supports the understanding and may provide further improvement of the absorbers. In this paper lateral inhomogeneities are studied by spatially resolved photoluminescence (PL) of the absorber, from which local quasi-Fermi level splitting and local absorbance are extracted.

2. Theory

The generalization of Planck's law has been previously used to describe the stationary PL of semiconductors and to determine opto-electronic properties e.g. the quasi-Fermi level splitting and absorbance [9, 10, 11]. For absorber layers with grainy structure optical and electronic properties are locally fluctuating and thus any analysis, including spectral PL, has to be recorded laterally resolved.

With a lateral varying splitting of the quasi-Fermi levels $E_{Fn}(x,y) - E_{Fp}(x,y)$ and absorbance $A(\hbar\omega, x, y)$ Planck's generalized law for the photon flux j_γ emitted by a sample reads [9]

$$j_\gamma(\hbar\omega, x, y) = Y_{PL}(\hbar\omega, x, y) = \frac{C \cdot A(\hbar\omega, x, y) \cdot (\hbar\omega)^2}{\exp\left(\frac{\hbar\omega - (E_{Fn}(x,y) - E_{Fp}(x,y))}{kT(x,y)}\right) - 1}, \tag{1}$$

in which $k, T(x,y), \hbar\omega$ and C represent Boltzmann constant, temperature, photon energy; the constant $C = (4\pi^2\hbar^3c^2)^{-1}$. The detected photon flux Y_{PL} includes calibration of detector signal and optical path.

For high photon energies, where $\hbar\omega - (E_{Fn}(x,y) - E_{Fp}(x,y)) \gg kT$, and the absorbance A approaches unity ($A \approx 1$) (1) can be written as

$$\begin{aligned} \ln\left(\frac{Y_{PL}(\hbar\omega, x, y)}{C \cdot (\hbar\omega)^2}\right) &= -\frac{\hbar\omega - (E_{Fn}(x,y) - E_{Fp}(x,y))}{kT(x,y)} \\ &= B(\hbar\omega, x, y), \end{aligned} \tag{2}$$

allowing for the determination of the splitting of the quasi-Fermi levels $E_{Fn}(x,y) - E_{Fp}(x,y)$ by a fit of the Bose term $B(\hbar\omega, x, y)$. According to [10] the absorbance $A(\hbar\omega, x, y)$ can be calculated as well by

$$\ln A(\hbar\omega, x, y) = \ln\left(\frac{Y_{PL}(\hbar\omega, x, y)}{C \cdot (\hbar\omega)^2}\right) - B(\hbar\omega, x, y). \tag{3}$$

This laterally varying absorbance $A(\hbar\omega, x, y)$ is examined for a CIS layer with respect to absorption $A_{def}(x, y)$ of sub bandgap states and the correlation of A_{def} to the local splitting of the quasi-Fermi levels $E_{Fn}(x, y) - E_{Fp}(x, y)$.

In our approach we assume that the quasi-Fermi level splitting $E_{Fn}(x, y) - E_{Fp}(x, y)$ varies only laterally and is fairly constant over the absorber thickness, since we perform the analyses under open circuit conditions, which provide for most "flat" carrier depth profile.

By numerical generation of PL signals including photon propagation, reflection at phase borders and interference effects, reabsorption, defect densities as well as depth dependent profiles of the band gap, we are able to study the influence of different profiles on the spectral behavior of the luminescence. And we conclude — mainly for the high photon energy wing of the PL — that in the vicinity of the heterojunction in the absorber in V_{oc} conditions no substantial departure from a "flat" profile of excess carrier concentration or say "flat" depth profile of the minority carrier quasi-Fermi level for reasonable parameters, e.g. surface recombination velocities $S < 10^4$cm s^{-1}, can be detected [12].

3. Experiment

In the work presented here, a $CuInS_2$ (CIS) thin-film absorber (2 μm) on a molybdenum back contact passivated with CdS (50 nm to 80 nm) is analysed. A detailed description of the absorber deposition process and properties has been published recently [3]. A solar cell with a nominally identical absorber reached an efficiency of about 9.5%. Grain sizes by AFM scans range from 1.5 μm to 2.5 μm [13]. The laterally and spectrally resolved PL spectra of the CIS sample are measured with a confocal microscope setup with resolution of $\triangle x \leq 1$ μm connected by a multimode fiber to a spectrograph and an optical multichannel analyzer (liquid nitrogen cooled InGaAs array) which allows to record a complete spectrum for each scanning point. To carry out laterally resolved scans samples are mounted on a piezo stage, e.g. reported recently for CIGSe [11, 14]. The sample is excited at room temperature with a laser at $\lambda = 532$ nm with 5×10^4 AM1.5 equivalent photon fluxes (10^{22}photons s^{-1}cm^{-2}). Since the confocal setup does not allow for an accurate calibration with respect to PL-photon fluxes collected from the sample, we detect lateral fluctuations of the quasi-Fermi level splitting $\triangle_{(x,y)}(E_{Fn} - E_{Fp})$ instead of the actual total splitting $E_{Fn}(x, y) - E_{Fp}(x, y) = \triangle_{(x,y)}(E_{Fn} - E_{Fp}) + \chi$ with an arbitrary but constant offset χ independent of x and y.

4. Results and Discussion

Figure 1 displays the integral PL yield $Y_{PL}(x, y)$ of the sample in a scan area of 50 μm $\times$ 50 μm corresponding to (250×250) spectra. Y_{PL} shows lateral fluctuations up to a factor of 10. Accompanied with strong spectral fluctuations exemplarily shown in figure 2 by three spectra, each spectrum consists of two peaks, one at about 1.5 eV which

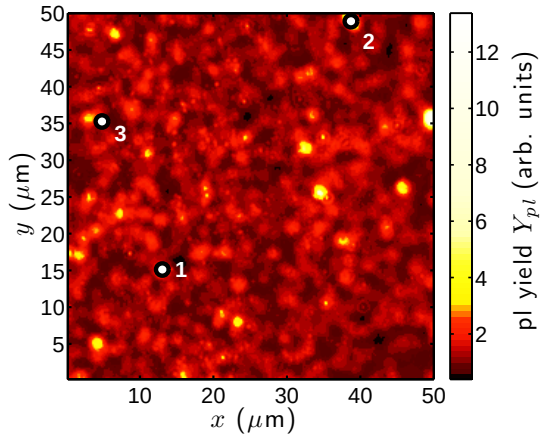

Figure 1. Entire photoluminescence (PL) yield obtained from a laterally resolved scan on $CuInS_2$ over a scan-area of 50 μm $\times$ 50 μm with excitation of 5×10^4 AM1.5 equivalent photon fluxes (10^{22} photons cm^{-2} s^{-1}) at $\lambda = 532$ nm. The spectra for the marked positions (1-3) are shown in figure 2.

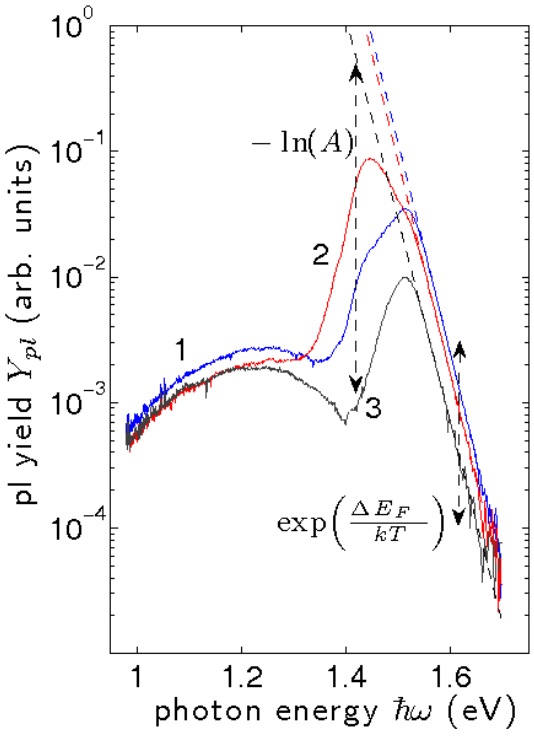

Figure 2. Individual PL spectra for positions in figure 1. The dashed line represents the linear regression according to (2). A variation in the splitting of the quasi-Fermi levels $\Delta E_F = \Delta_{(x,y)}(E_{Fn} - E_{Fp})$ results in a variation of the high energy PL wing (arrows at r.h.s.). The difference between the dashed line (Bose term) and spectral luminescence $Y_{PL}(\hbar\omega)$ in the low photon energy regime represents the spectral absorption ($\propto -\ln A$).

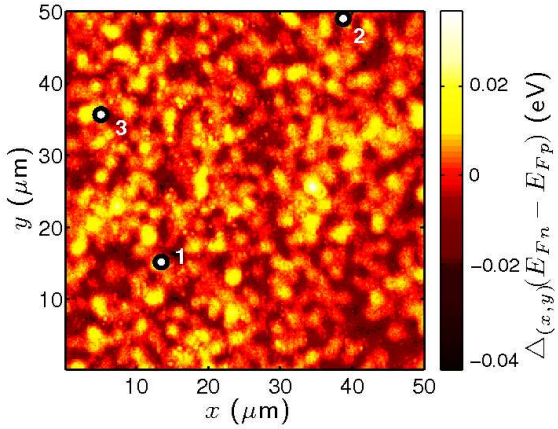

Figure 3. Lateral mapping of the fluctuation in splitting of quasi-Fermi levels obtained from equation (2) from a laterally resolved photoluminescence scan on $CuInS_2$ (data set of figure 1). Individual spectra of marked positions (1-3) shown in figure 2.

is due to band-to-band recombination and another one at approximately 1.2 eV which we assign to defect recombination [15]. As can be seen from the three exemplary spectra the ratio between the high energy peak and the low energy peak varies with the lateral position. From the spectral PL $Y_{PL}(\hbar\omega)$ we derive $\triangle_{(x,y)}(E_{Fn}-E_{Fp})$ and $T(x,y)$ by the high energy wing, whereas the absorbance $A(\hbar\omega,x,y)$ is determined from low energy photons. Consequently the integrated PL yield is inappropriate for a comprehensive interpretation of these magnitudes. The relative splitting $\triangle_{(x,y)}(E_{Fn}-E_{Fp})$ has been calculated according to (2) (dashed lines in figure 2). For each individual spectrum ranges for fitting $\triangle_{(x,y)}(E_{Fn}-E_{Fp})$ and temperature $T(x,y)$ have been selected appropriately with respect to noise level and negligible departure of absorbance $A(x,y)=1$.

Figure 3 shows this $\triangle_{(x,y)}(E_{Fn}-E_{Fp})$ for the same scan presented in figure 1 by the integral PL yield. Variations up to 80 meV have been observed with structure sizes in the range of $1-2$ μm. An analysis of structure sizes by Minkowski opening operations in maps of quasi-Fermi level splitting and AFM surface contour on similar absorber layers has been published [13]. Grain sizes in AFM topography range from 1.5 μm to 2.5 μm, between surface contour and $\triangle_{(x,y)}(E_{Fn}-E_{Fp})$ no correlation has been detected.

To quantify the above mentioned variation in $\triangle_{(x,y)}(E_{Fn}-E_{Fp})$ the frequency of occurrence f is plotted versus its relative value (figure 4). The small inset shows the variations in the inverse slope "kT". The range of variations results in a full width at half maximum ($\mathrm{FWHM}_{\triangle E_F}$) of about 30 meV, being larger than $\mathrm{FWHM}_{\triangle E_F}$ in CIGSe of 15 meV [11, 16].

According to (3) the local absorbance for each of the spectra has been calculated and exemplary spectra are shown in figure 5 in a semi-logarithmic plot for the positions marked in figures 1 and 3. Between 1 eV and 1.6 eV the absorbance spans over ten orders of magnitude showing a substantial absorption in the sub bandgap regime.

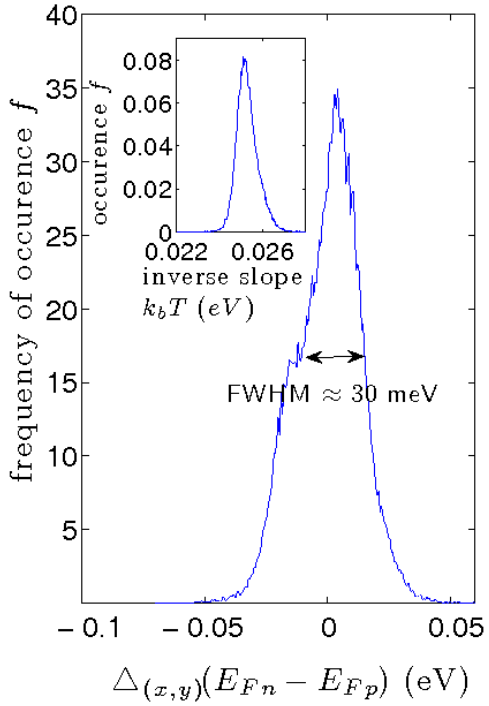

Figure 4. Frequency of occurrence f of fluctuation of the splitting of quasi-Fermi level for a $CuInS_2$ sample ($\triangle_{(x,y)}(E_{Fn} - E_{Fp})$ from data in figure 3). With $FWHM_{\triangle E_F}$ of about 30 meV. The inset shows the variations in the inverse slope kT.

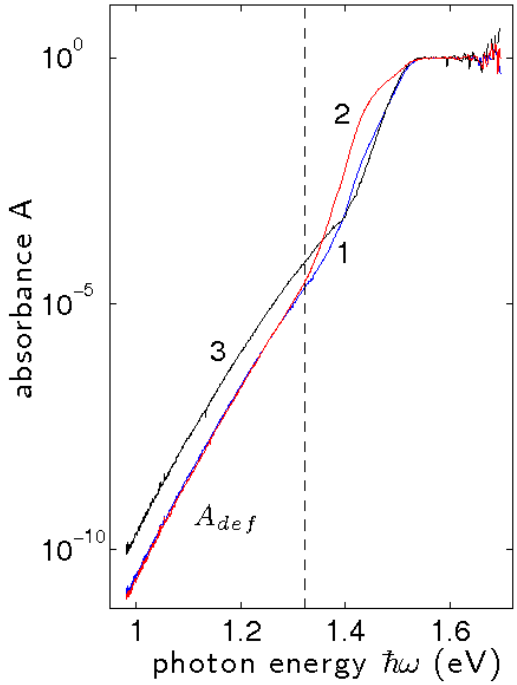

Figure 5. Spectral absorbance of a CIS thin film calculated from the spectral photoluminescence for individual positions (1-3) in figures 1, 3 and 6. The absorbance of defect states A_{def} is defined by $A_{def}(x,y) = \int_{\hbar\omega=1eV}^{1.35eV} A(\hbar\omega, x, y)\mathrm{d}\hbar\omega$.

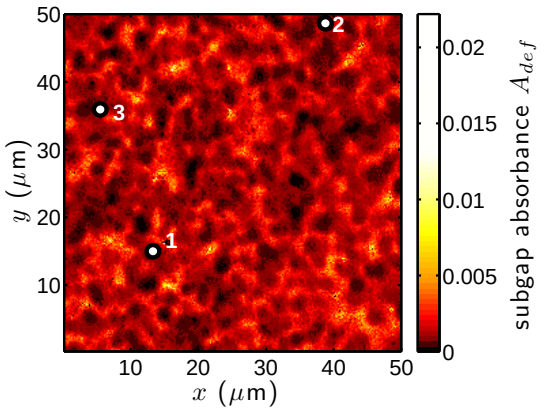

Figure 6. Mapping of defect absorbance $A_{def}(x,y) = \int_{\hbar\omega=1eV}^{1.35eV} A(\hbar\omega,x,y)\mathrm{d}\hbar\omega$ of a CIS absorber evaluated according to equations 3 and 4.

In order to correlate the absorbance spectra to the local splitting of the quasi-Fermi levels $\triangle_{(x,y)}(E_{Fn} - E_{Fp})$ the sum of the absorbance in the low energy range (1 eV $< \hbar\omega <$ 1.35 eV) defined as the absorbance via defect states

$$A_{def}(x,y) = \int_{\hbar\omega=1eV}^{1.35eV} A(\hbar\omega,x,y)\mathrm{d}\hbar\omega \tag{4}$$

has been evaluated and is shown in a (50×50) μm^2 mapping in figure 6 in arbitrary numbers.

For $A_{def}(x,y)$ we find similar structure sizes as for figure 3. $\triangle_{(x,y)}(E_{Fn} - E_{Fp})$ and A_{def} show a clear anti-correlation with a correlation coefficient of $r = -0.85$ with $r \in [-1,1]$. This indicates a lowering of the local quasi-Fermi level splitting by increase in local sub bandgap defects obviously due to a considerable contribution of these defects to recombination. It has to be noted that no direct correlation between $Y_{PL,def}(x,y) = \int_{\hbar\omega=1eV}^{1.35eV} Y_{PL}(\hbar\omega,x,y)\mathrm{d}\hbar\omega$ and $\triangle_{(x,y)}(E_{Fn} - E_{Fp})$ occurs since a change in the quasi-Fermi level splitting leads to a change in the overall PL yield as described by (1); in other words, if $A_{def}(x,y)$ was constant an increase in $E_{Fn}(x,y) - E_{Fp}(x,y)$ would result in a higher luminescence yield and a higher $Y_{PL,def}(x,y)$. A separation of these two competing effects, as it is carried out by the calculation of the local absorbance, is therefore necessary. A similar anti-correlation between $A_{def}(x,y)$ and $\triangle_{(x,y)}(E_{Fn} - E_{Fp})$ has also been found for numerous CIS and CIGS absorbers.

5. Summary

The laterally and spectrally resolved PL spectra of CIS samples show inhomogeneities in quasi-Fermi level splitting in the length scale of a few microns. The variations in $\triangle_{(x,y)}(E_{Fn} - E_{Fp})$ are found to have a full width at half maximum of 30 meV which is much larger than that reported for CIGSe samples. By applying Planck's generalized law it is possible to determine the local absorbance of the layer and to identify a sub

bandgap absorbance $A_{def}(x, y)$ with a strong anti-correlation to the local quasi-Fermi level splitting indicating that $\triangle_{(x,y)}(E_{Fn} - E_{Fp})$ and thereby the open circuit voltage of the final cell eV_{oc} is strongly governed by recombination via deep defects.

Acknowledgments

The authors like to thank P. Pargmann for technical support and the Helmholtz Zentrum Berlin, SE2 for sample preparation. Furthermore financial support of the BMU under contract no. 0327 589-C (KD-CIS) is gratefully acknowledged.

References

[1] Repins I., Contreras M.A., Egaas B., DeHart C., Scharf J., Perkins C.L., To B. and Noufi R. 2008 *Prog. Photovolt: Res. Appl.* **16** 235239.
[2] Klenk R., Klaer J., Scheer R., Lux-Steiner M.C., Luck I., Meyer N. and Rühle U. 2005 *Thin Solid Films* **480** 509-514.
[3] Klaer J., Klenk R. and Schock H.W. 2007 *Thin Solid Films* **515** 15, 5929-5933.
[4] Kaigawa R., Neisser A., Klenk R. and Lux-Steiner M.-Ch. 2002 *Thin Solid Films* **415** 266-271.
[5] Siemer K., Klaer J., Luck I., Bruns J., Klenk R., and Bräunig D. 2001 *Sol. Energy Mater. Sol. Cells* **67** 159166.
[6] Ellmer K., Hinze J., and Klaer J. 2002 *Thin Solid Films* **413** 92-97.
[7] Bothe K., Bauer G.H. and Unold T. 2002 *Thin Solid Films* **403-404** 453-456.
[8] Taretto K. and Rau U. 2008 *J. Appl. Phys.* **103** 094523.
[9] Würfel P. 1982 *J. Phys. C: Solid State Phys.* **15** 3967-3985.
[10] Daub E. and Würfel P. 1995 *Phys. Rev. Lett.* **74** 1020-1023.
[11] Gütay L. and Bauer G.H. 2009 *Thin Solid Films* **517** 2222-2225.
[12] Knabe S., Gütay L. and Bauer G.H. 2009 *Thin Solid Films* **517** 2344-2348; Knabe S, Bauer G.H. 2010 *E-MRS conf. session M* submitted.
[13] Heidemann F., Gütay L., Meeder A., Bauer G.H. 2009 *Thin Solid Films* **517** 2427-2430.
[14] Gütay L. and Bauer G.H. 2007 *Thin Solid Films* **515** 6212-6216.
[15] Unold T., Sieber I. and Ellmer K. 2006 *Appl. Phys. Lett.* **88** 213502.
[16] Gütay L., Pomraenke R., Lienau C. and Bauer G.H. 2009 *Phys. Status Solidi A* **206** 1005-1008.